Small clusters with anisotropic antiferromagnetic exchange in a magnetic field

2004 J. Phys.: Condens. Matter 16 2407

(http://iopscience.iop.org/0953-8984/16/13/019)

INSTITUTE OF PHYSICS PUBLISHING JOURNAL OF PHYSICS: CONDENSED MATTER

J. Phys.: Condens. Matter **16** (2004) 2407–2419 PII: S0953-8984(04)75245-5

Small clusters with anisotropic antiferromagnetic exchange in a magnetic field

J B Parkinson[1], **R J Elliott**[2] **and J Timonen**[3]

[1] Mathematics Department, UMIST, PO Box 88, Sackville Street, Manchester M60 1QD, UK
[2] Theoretical Physics, 1 Keble Road, Oxford OX1 3NP, UK
[3] Department of Physics, University of Jyväskylä, PO Box 35, FIN-40351 Jyväskylä, Finland

Received 23 January 2004
Published 19 March 2004
Online at stacks.iop.org/JPhysCM/16/2407 (DOI: 10.1088/0953-8984/16/13/019)

Abstract

We consider small symmetric clusters of magnetic atoms (spins) with anisotropic exchange interaction between the atoms in a magnetic field at zero temperature. The inclusion of the anisotropy leads to a wealth of different phases as a function of the applied magnetic field. These are not phases in the thermodynamic sense with critical properties but rather physical structures with different arrangements of the spins and hence different symmetries. We study the spatial symmetry of these phases, for the classical and quantum cases. Results are presented mainly for three frustrated systems, the triangle, the tetrahedron and the five-atom ring, which have many interesting features. In the classical limit we obtain phase diagrams in which some of the phase changes occur because of energy crossings and others due to energy bifurcations, corresponding to 'first-' and 'second-order' changes. In the quantum case we show how the symmetries of the states are related to the corresponding classical symmetries.

(Some figures in this article are in colour only in the electronic version)

1. Introduction

In two recent papers we have studied small symmetric clusters of magnetic atoms with isotropic antiferromagnetic exchange in a magnetic field. In the first of these papers [1] we looked at clusters with sizes from eight (octahedral) to 19 (fcc) atoms. We observed phase changes in the classical zero-temperature magnetization curve but we were not able to correlate these with changes in the quantum ground states in any convincing manner. Note that we refer to 'phase changes' although of course these are not thermodynamic phase changes but rather changes between states of different symmetry at $T = 0$ as the applied magnetic field B is varied.

In the second paper [2] we looked mainly at smaller clusters (sizes two to eight atoms), again with isotropic exchange. Here we were able to study two things. Firstly we studied the quantum to classical transition as $S \to \infty$ during which the steps of the quantum magnetization curve become progressively smaller. In the limit one obtains the piecewise smooth classical

magnetization curves. Secondly we studied the spatial symmetry of the quantum states and as a result were able to characterize the symmetry of the classical configurations as the limit of these. Typically we find that a given quantum state has a symmetry which can be described in terms of the irreducible representations of the space group of the cluster. The classical symmetry is usually lower (i.e. a combination of more irreducible representations), since several quantum states with different symmetries contribute to the smooth classical curve.

The situation in the case of the three- and four-atom clusters is complicated by the presence of additional symmetry which is 'hidden' as far as the space group is concerned but is clear from the fact that the Hamiltonian in these cases can be factorized. The low-lying states, which are the only ones relevant to the zero-temperature magnetization curve, can then be written in terms of effective spins formed from linear combinations of two or more actual spins. The effect of this is to introduce extra massive degeneracies into the low-lying energy levels when the exchange is isotropic. A full treatment of the energy levels for the special case of a triangle of $S = 3/2$ Cr atoms was given earlier by Bates and Jasper [3].

In this paper we focus mainly on three small frustrated clusters, the triangle, the tetrahedron and the five-atom ring. The five-atom ring is the smallest non-trivial cluster for which no factorization occurs. Most importantly we introduce anisotropy into the exchange. This has the effect of causing phase changes as the magnetic field changes even for small clusters. We shall study the symmetry of these different phases and the transitions between them. This has enabled us to understand the symmetry of the classical states in terms of the irreducible representations of the space group as well as the way in which these are formed from the quantum states in the $S \to \infty$ limit.

Small clusters of spins have become active topics of experimental and theoretical research since the recent discoveries of magnetic molecular complexes. This work has been extensively reviewed by Winpenny and Rawson [4, 5]. Large molecules of Fe_8 and of Mn_{12} acetate type have a large total spin, typically of the order of $S = 10$, and a large energy barrier against spin rotation. These properties have made them ideal for studying quantum relaxation [6–9]. In view of the problems addressed in this article, more interesting compounds are however those molecular complexes in which there is no such energy barrier. An example of that kind of molecule is the V_{15} polyoxovanadate [10]. In this molecule the 15 vanadium atoms with spin $S = 1/2$ form a structure composed of a triangle sandwiched in between two hexagons. All exchange interactions between spins are antiferromagnetic. Because of the relative strengths of these interactions the low-energy magnetic excitations of the molecule can be described by three spins $S = 1/2$ with antiferromagnetic coupling [11, 12]. The magnetization curve of this molecule at low temperatures has stepwise structure similar to the triangle of $S = 1/2$ spins studied below. The more detailed magnetic structure of the system only shows up at higher energies, and has not been analysed experimentally. As similar magnetic molecules are likely to be constructed in the near future, we believe that our methods will be useful in analysing the magnetic properties of small clusters of spins with antiferromagnetic coupling.

2. Triangle of spin-S atoms

The Hamiltonian with XXZ-type anisotropic exchange and the magnetic field in the z-direction is

$$\mathcal{H} = J_z \sum_{i=1}^{3} s_i^z s_{i+1}^z + J_x \sum_{i=1}^{3} (s_i^x s_{i+1}^x + s_i^y s_{i+1}^y) - B \sum_{i=1}^{3} s_i^z. \tag{1}$$

For $J_x = J_z (= J)$ this Hamiltonian factorizes in the form

$$\mathcal{H} = \frac{J}{2}(\mathbf{t} \cdot \mathbf{t} - 3S^2) - Bt^z$$

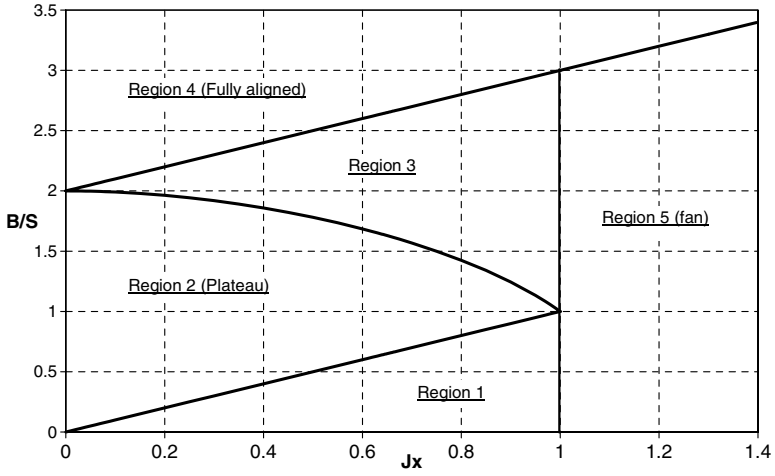

Figure 1. The $T = 0$ phase diagram of the classical triangle with $J_z = 1$ as a function of B and J_x.

where $\mathbf{t} = \mathbf{s}_1 + \mathbf{s}_2 + \mathbf{s}_3$. This was noted in our earlier paper and corresponds to a hidden symmetry for this case, which results in massive degeneracy. The inclusion of the anisotropy in equation (1) largely removes this degeneracy. We shall choose $J_z = 1$, allowing J_x to vary.

Classically we obtain the lowest energy for each J_z, J_x, B by starting with a random set of orientations for the spins and then using a Powell method [16] to relax the system into its lowest-energy (zero-temperature) configuration. We find five distinct regions which are conveniently described in terms of the orientation angles θ, ϕ, given in the following table.

	Region 1		Region 2		Region 3		Region 4		Region 5	
Atom	θ	ϕ	θ	ϕ	θ	ϕ	θ	ϕ	θ	ϕ
1	θ_1	0	0	—	θ_1	0	0	—	θ_1	0
2	θ_1	π	0	—	θ_1	0	0	—	θ_1	$2\pi/3$
3	π	—	π	—	θ_2	π	0	—	θ_1	$4\pi/3$

Since we are using the spin-space group [13] where different symmetry transformations can be applied separately to the spin and space configurations we note that the energies are invariant under two trivial sets of operations:

(i) an arbitrary uniform rotation of the spins about the z-axis and
(ii) any permutation of the atoms corresponding to an element of the space group C_{3v}.

In this model the axis of symmetry applied to the spins in (i) can be chosen independently of the axes of the triangle—although in real systems they would normally be coincident.

The phase diagram is shown in figure 1. The boundary between regions 1 and 2 is given by $B_{12} = SJ_x$ and between regions 2 and 3 by

$$B_{23} = S/2\left[J_z - J_x + \sqrt{4J_z^2 + 4J_xJ_z - 7J_x^2}\right].$$

All the boundaries between regions are examples of bifurcations in the energy versus B curves and the values for the orientation angles are continuous across the boundaries. The

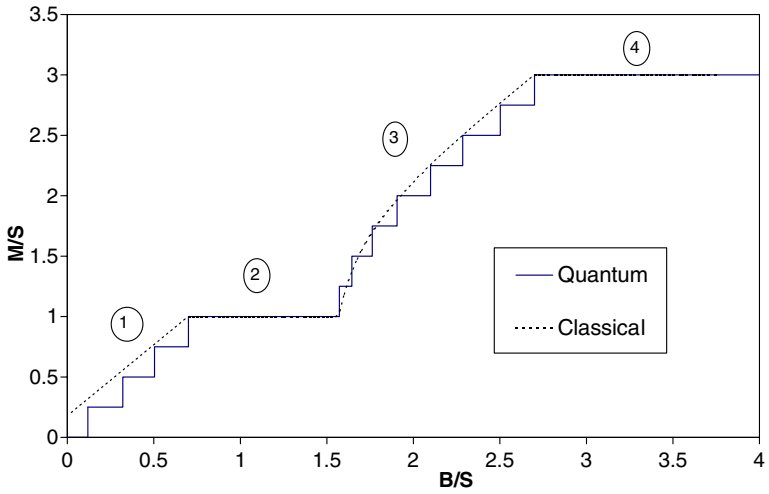

Figure 2. Magnetization curve of the triangle for $J_z = 1$, $J_x = 0.7$ as a function of B, indicating the different regions. The stepped curve is the corresponding quantum curve for $S = 4$.

only exception is the $J_x = J_z$ boundary (for all $B < 3SJ_z$) at which level crossing takes place. This is also the boundary with the massive degeneracy.

The magnetizations in the five regions are given in the following table using $m = M/S$ and $b = B/S$. In region 3 the magnetization has only been found numerically.

Region	Magnetization, m
1	$[2b + (J_z - J_x)]/[J_z + J_x]$
2	1
4	3
5	$3b/(2J_z + J_x)$

Region 4 is the fully aligned region which exists for all $B \geqslant S(J_x + 2J_z)$. Region 5 is a fanlike structure occurring for $J_x \geqslant J_z$ and $B < S(J_x + 2J_z)$. Region 2 we refer to as the plateau region because of the form of the magnetization curve. This magnetization plateau at $M = S$ is not related to the magnetization plateau discussed by Oshikawa *et al* [15] which is due to collective excitations in a system with a large number of atoms. Rather it is a precursor of the Ising stepped magnetization curve obtained for $J_x = 0$.

The magnetization curve for $J_x = 0.7$, $J_z = 1.0$ is shown in figure 2 which also shows the quantum curve for $S = 4$ for comparison.

The classical symmetries are obtained in terms of the irreducible representations of the space group C_{3v} [14] as follows. In each case we determine which of the group operations leave the configuration unchanged. No changes in spin orientation are allowed. This gives the characters of the representation and hence from the character table we obtain the corresponding combination of irreducible representations.

In region 4 all spins are parallel so the configuration is invariant under all group operations and the representation is Γ_1. In regions 1 and 5 all spins are oriented in different directions so that under the operations of the *space* group only the identity leaves it invariant. This corresponds to the regular representation $\Gamma_1 + \Gamma_2 + 2\Gamma_3$. In regions 2 and 3 two spins are parallel so the configuration is invariant under the identity and one of the three σ_v operations

leading to the representation $\Gamma_1+\Gamma_3$. Clearly regions 1 and 5 and regions 2 and 3 are physically distinct but this would only lead to different representations if the spin-space group were used rather than the space group.

Quantum mechanically we have obtained the lowest eigenstates for each value of M and from these we can obtain the symmetries. The magnetization curves now consist of a series of steps as states with different magnetizations and symmetries become lowest as a function of B. An example is shown for the case $J_z = 1$, $J_x = 0.7$ and $S = 4$ in figure 2.

We find that region 4 is Γ_1 as expected and in region 3 the steps in the magnetization alternate between Γ_1 and Γ_3, consistent with the classical result. In region 1 we find that the steps alternate between Γ_1 and Γ_2 for integer S, and are always Γ_3 for integer $+\frac{1}{2}$. Taken together, this combination is consistent with the classical result $\Gamma_1 + \Gamma_2 + 2\Gamma_3$. In region 2 we find Γ_1 for integer S and Γ_3 for integer $+\frac{1}{2}$, again consistent.

Although in this case consideration of the ground states of both the integer and integer $+\frac{1}{2}$ together leads directly to the correct classical representation, this is not always true. The classical limit is correctly obtained in the limit $S \to \infty$. One should therefore look at all low-lying states in this limit to determine which become degenerate with the ground state. Because the states of different symmetry are ordered differently for the integer and integer $+\frac{1}{2}$ it may happen that all the states which become degenerate in the $S \to \infty$ limit occur as ground states of one or the other as here. However, we have observed other cases where some low-lying states which become degenerate with the ground state in this limit do not occur as ground states for finite S for either integer or integer $+\frac{1}{2}$, and the true classical representation is obtained only when these states are included.

An example of this is in region 5 where we find that the steps form a sequence with symmetries $\Gamma_1, \Gamma_3, \Gamma_3, \Gamma_2, \Gamma_3, \Gamma_3, \Gamma_1, \Gamma_3, \Gamma_3, \Gamma_2, \ldots$ for both integer and integer $+\frac{1}{2}$. This would imply a representation of the form $\Gamma_1 + \Gamma_2 + 4\Gamma_4$, which is clearly not the regular representation. We believe that the explanation for this is that steps with symmetry Γ_1 occur because the lowest lying eigenstate has this symmetry but that there is another low-lying state with symmetry Γ_2. The classical representation is obtained in the limit $S \to \infty$ and, provided the low-lying state becomes degenerate with the lowest in this limit, the step would have symmetry $\Gamma_1 + \Gamma_2$. A similar argument applies to the Γ_2 steps which also become $\Gamma_1 + \Gamma_2$ in this limit. The final result is the regular representation, as for the classical case.

3. Tetrahedron of spin-S atoms

The Hamiltonian with anisotropic exchange is

$$\mathcal{H} = J_z[s_1^z s_2^z + s_1^z s_3^z + s_1^z s_4^z + s_2^z s_3^z + s_2^z s_4^z + s_3^z s_4^z] + J_x[s_1^x s_2^x + s_1^x s_3^x + s_1^x s_4^x + s_2^x s_3^x + s_2^x s_4^x + s_3^x s_4^x] + J_x[s_1^y s_2^y + s_1^y s_3^y + s_1^y s_4^y + s_2^y s_3^y + s_2^y s_4^y + s_3^y s_4^y] + B\sum_{i=1}^{4} s_i^z. \tag{2}$$

For $J_x = J_z(= J)$ this Hamiltonian factorizes in the form

$$\mathcal{H} = \frac{J}{2}(\mathbf{t}\cdot\mathbf{t} - 4S^2) - Bt^z$$

where $\mathbf{t} = \mathbf{s}_1 + \mathbf{s}_2 + \mathbf{s}_3 + \mathbf{s}_4$. This is a similar factorization to the triangle and corresponds to a hidden symmetry for this case also, again resulting in massive degeneracy. Just as for the triangle the inclusion of the anisotropy in equation (2) largely removes this degeneracy. Again we take $J_z = 1$, allowing J_x to vary.

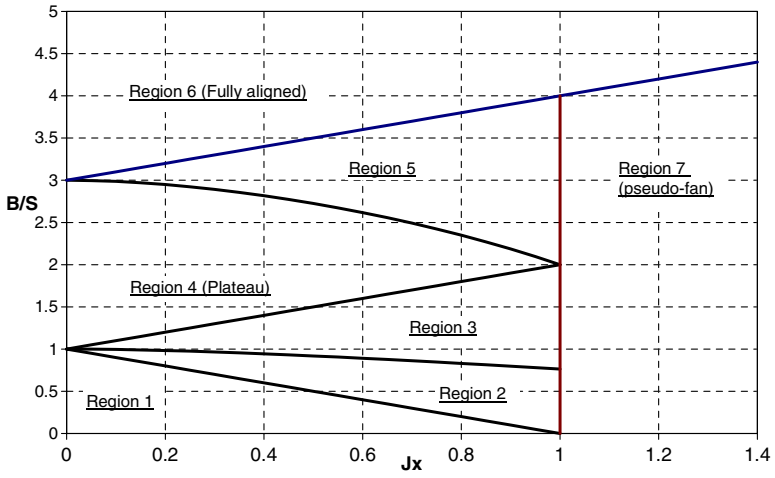

Figure 3. The $T = 0$ phase diagram of the classical tetrahedron with $J_z = 1$ as a function of B and J_x.

Classically we find seven distinct regions with orientation angles θ, ϕ shown in the following table.

	Region 1		Region 2		Region3		Region 4		Region 5		Region 6		Region 7	
Atom	θ	ϕ	θ	ϕ	θ	ϕ	θ	ϕ	θ	ϕ	θ	ϕ	θ	ϕ
1	0	—	0	—	θ_1	0	0	—	θ_1	0	0	—	θ_1	0
2	0	—	0	—	θ_1	0	0	—	θ_1	0	0	—	θ_1	π
3	π	—	θ	0	θ_2	0	0	—	θ_1	0	0	—	θ_1	ϕ_1
4	π	—	$-\theta$	0	θ_3	0	π	—	θ_2	0	0	—	θ_1	$\pi + \phi_1$

The value of ϕ_1 in region 7 is arbitrary since the energy in this region is independent of it. Region 6 is the fully aligned region which exists for all J_x, J_z provided $B > S(3J_z + J_x)$. The classical phase diagram is shown in figure 3. Along the boundary at $J_x = J_z$ the massive degeneracy referred to earlier occurs.

The crossover fields between the different regions are given in the following table using the notation B_{ij} for the crossover field between regions i and j, and $b_{ij} = B_{ij}/S$. b_{23} is only known numerically and is not shown.

i, j	b_{ij}
1, 2	$J_z - J_x$
3, 4	$J_z + J_x$
4, 5	$2J_z - J_x + \sqrt{J_z^2 + 2J_zJ_x - 2J_x^2}$
5, 6	$3J_z + J_x$
7, 6	$3J_z + J_x$

All the boundaries are examples of energy bifurcations except the $J_x = J_z$ boundary.

The magnetizations $m = M/S$ of the different regions as a function of $b = B/S$ are given in the following table. For the regions which are not shown the magnetization would

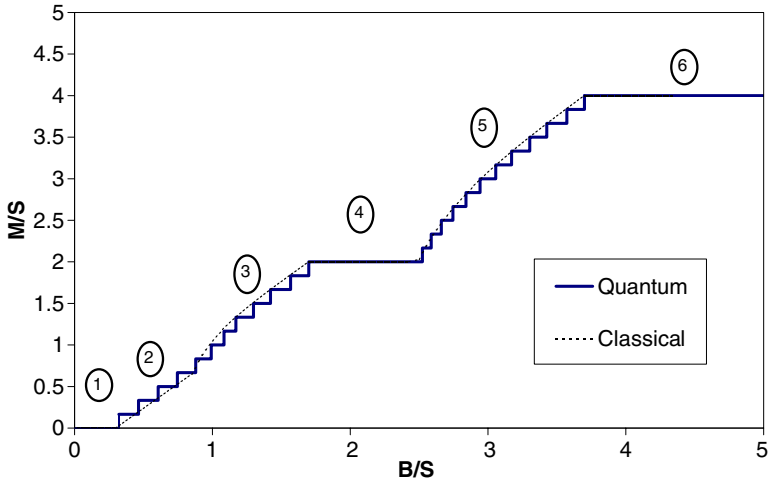

Figure 4. Magnetization curve of the tetrahedron for $J_z = 1$, $J_x = 0.7$ as a function of B, indicating the different regions. The stepped curve is the corresponding quantum curve for $S = 6$.

be obtained as the solution of a cubic or higher order equation and has only been found numerically.

Region	Magnetization, m
1	0
2	$2(b + J_x - J_z)/(J_x + J_z)$
4	2
6	4
7	$4b/(3J_z + J_x)$

The magnetization curve for $J_x = 0.7$, $J_z = 1.0$ is shown in figure 4, which also shows the quantum result for $S = 6$.

The classical symmetries are obtained in terms of the irreducible representations of the space group T_d as follows. In region 6 all spins are parallel ($aaaa$) so the configuration is invariant under all group operations and the representation is Γ_1. In region 1 two pairs of spins are parallel ($aabb$) with representation $\Gamma_1 + \Gamma_3 + \Gamma_5$. In regions 2 and 3 only two of the four spins are parallel ($aabc$) with representation $\Gamma_1 + \Gamma_3 + \Gamma_4 + 2\Gamma_5$. In regions 4 and 5 three spins are parallel ($aaab$) with representation $\Gamma_1 + \Gamma_5$. Finally in region 7 all spins are in different directions ($abcd$) giving the regular representation $\Gamma_1 + \Gamma_2 + 2\Gamma_3 + 3\Gamma_4 + 3\Gamma_5$. Regions 2 and 3 and regions 4 and 5 would be distinguished if the spin space group were used.

We find that the symmetries of the lowest quantum eigenstates for each value of M are consistent with the classical picture. However, in any region one obtains a subset of the classical representations, e.g. in regions 2 and 3 for $S = 6$ we obtain alternating Γ_1 and Γ_4. The full classical representation is usually obtained by considering both integer and integer $+\frac{1}{2}$ values of S. In some cases missing representations exist in low-lying states which become degenerate with the lowest state as $S \to \infty$.

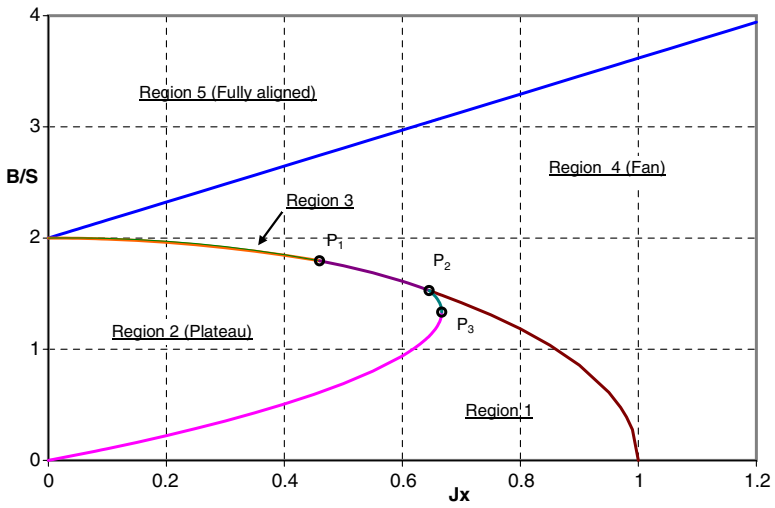

Figure 5. The $T = 0$ phase diagram of the classical five-atom ring with $J_z = 1$ as a function of B and J_x.

4. Five-atom ring of spin-S atoms

The Hamiltonian with anisotropic exchange is

$$\mathcal{H} = J_z \sum_{i=1}^{5} s_i^z s_{i+1}^z + J_x \sum_{i=1}^{5} (s_i^x s_{i+1}^x + s_i^y s_{i+1}^y) - B \sum_{i=1}^{5} s_i^z. \tag{3}$$

We shall choose $J_z = 1$. Note that this Hamiltonian does not factorize.

Classically we find five distinct regions with orientation angles θ, ϕ shown in the following table.

	Region 1		Region 2		Region 3		Region 4		Region 5	
Atom	θ	ϕ	θ	ϕ	θ	ϕ	θ	ϕ	θ	ϕ
1	θ_1	0	0	—	θ_1	0	θ_1	0	0	—
2	θ_1	π	0	—	θ_1	0	θ_1	$4\pi/5$	0	—
3	θ_2	0	π	—	θ_2	π	θ_1	$8\pi/5$	0	—
4	0	—	0	—	θ_3	0	θ_1	$12\pi/5$	0	—
5	θ_2	π	π	—	θ_2	π	θ_1	$16\pi/5$	0	—

We refer to region 2, which has constant magnetization $M = S$, as the 'plateau' region because of the form of the magnetization curve in the cases in which it occurs. Region 4 is referred to as the 'fan' because of the arrangement of the spins, and region 5, with constant magnetization $M = 5S$, is the fully aligned region. The classical phase diagram is shown in figures 5 and 6.

The three special points marked have coordinates (J_x, b) as follows.

$P_1 = (0.459\,65, 1.794\,94)$ is the 'triple point' of regions 2, 3, 4.
$P_2 = (0.645\,45, 1.527\,88)$ is the 'triple point' of regions 1, 2, 4.
$P_3 = (2/3, 4/3)$ is the point at which region 2 has the largest possible value of J_x.

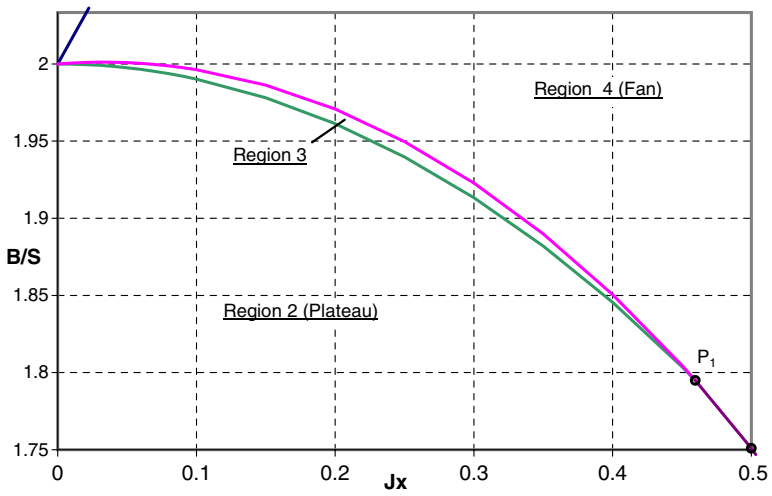

Figure 6. Enlarged portion of figure 5 showing region 3.

Note that neither of the boundaries of region 3 (see figure 6) is an analytic continuation of the line P_1P_2 nor is the line from P_2 to $(1, 0)$. Also note that there is no boundary at $J_x = J_z$ and no degeneracy along this line, associated with the fact that the Hamiltonian does not factorize.

The crossover fields for which analytic expressions have been found are given in the following table.

i, j	b_{ij}
1, 2	$\frac{1}{2}\left[(J_x + 2J_z) \pm \sqrt{(J_x + 2J_z)(2J_z - 3J_x)}\right]$
2, 4	$\frac{2}{5}\left[X + 2\sqrt{10J_zX - 6X^2}\right]$
4, 5	$2X$

where

$$X = J_z + \frac{(1+\sqrt{5})}{4} J_x. \tag{4}$$

Note that the boundary between regions 1 and 2 requires the $-$ sign from $(0, 0)$ to P_3 and the $+$ sign from P_2 to P_3. The boundary between regions 2 and 4 extends from P_1 to P_2. All other boundaries can be expressed in terms of cubic or quadratic equations and have only been obtained numerically.

In this case the boundaries at which the magnetization is discontinuous, namely B_{14}, B_{24} and B_{34}, are examples of level crossings. All other boundaries are examples of level bifurcations.

We show in figures 7–9 the magnetization M for $J_z = 1$ as a function of applied field B for various values of J_x.

The magnetization curve in region 4 is a straight line $m = 5b/2X$. Magnetization curves in regions 1 and 3 are complicated, involving solutions of quartic or cubic equations respectively. For $J_z \leqslant J_x$ only regions 4 and 5 occur, with the boundary given by $B = 2SX$.

From the observed arrangement of the spins in the cluster we can determine the symmetry in terms of the irreducible representations of the *space* group of the cluster C_{5v}. We shall use the symmetry group C_{5v} although an isomorphic permutation subgroup would strictly be more appropriate. We consider the five regions separately.

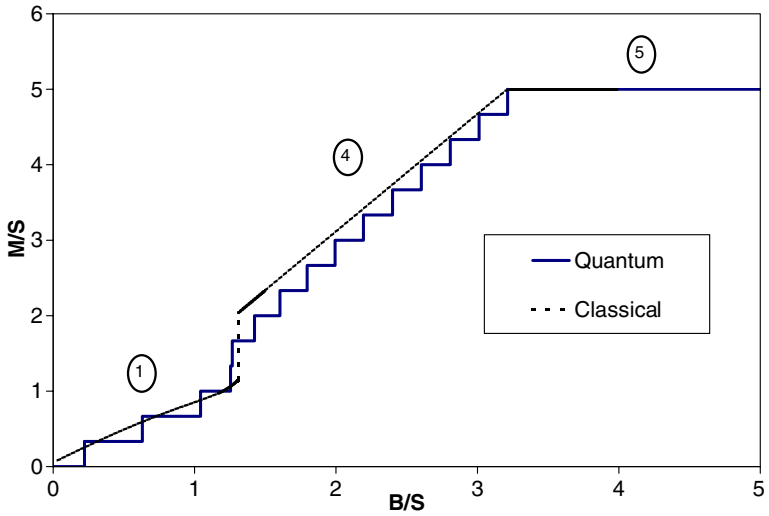

Figure 7. The $T = 0$ magnetization curve of the classical and $S = 3$ quantum five-atom ring as a function of B for $J_x = 0.75$. The plateau, region 2, is not observed in this case.

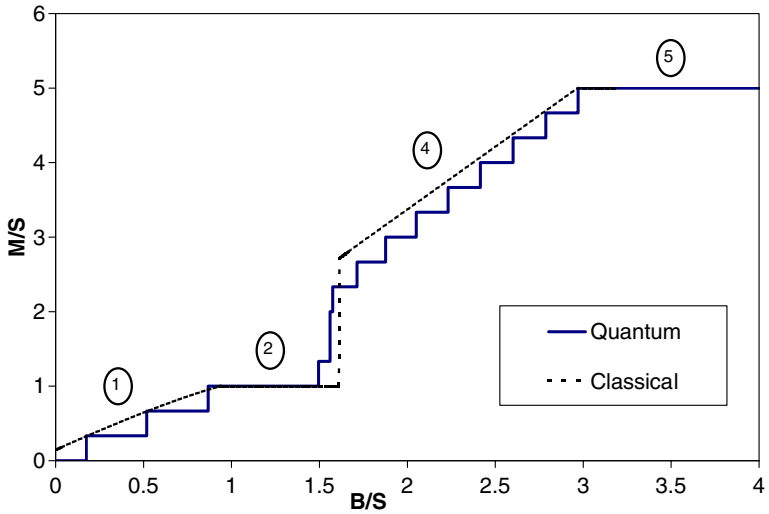

Figure 8. The $T = 0$ magnetization curve of the classical and $S = 3$ quantum five-atom ring as a function of B for $J_x = 0.6$.

For region 1 the table of orientation angles shows that no spins are parallel. Consequently, none of the operations of the space group leave the configuration unchanged except the identity, leading to the regular representation $\Gamma_1 + \Gamma_2 + 2\Gamma_3 + 2\Gamma_4$. For region 2 three spins are parallel and two are antiparallel. This is unchanged under the identity and one of the five σ_v operations. The representation is $\Gamma_1 + \Gamma_3 + \Gamma_4$. For region 3 there are two pairs of parallel spins and one other. Again the identity and one σ_v operation (the one where the axis passes through the odd spin) leave this unchanged, so again we obtain $\Gamma_1 + \Gamma_3 + \Gamma_4$.

For region 4 none of the spins are parallel so, as for region 1, we obtain the regular representation $\Gamma_1 + \Gamma_2 + 2\Gamma_3 + 2\Gamma_4$. As noted previously the operations of the space group

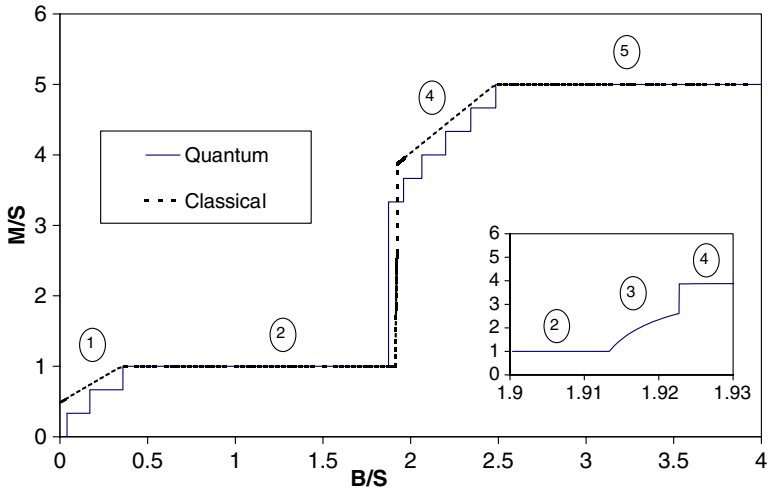

Figure 9. The $T = 0$ magnetization curve of the classical and $S = 3$ quantum five-atom ring as a function of B for $J_x = 0.3$. The enlargement shows the part of the curve corresponding to region 3.

leave the directions of the spins unchanged. Clearly a *combination* of a C_5 operation with a rotation of the spins by $4\pi/5$ would leave the configuration unchanged, but this would require use of the spin-space group rather than the space group considered here. We intend to investigate spin rotations in later work.

Finally, for region 5 all spins are parallel. The configuration is invariant under all the group operations so the representation is the identity representation Γ_1.

These classical symmetries are summarized in the following table.

Region	Symmetry
1	$\Gamma_1 + \Gamma_2 + 2\Gamma_3 + 2\Gamma_4$
2	$\Gamma_1 + \Gamma_3 + \Gamma_4$
3	$\Gamma_1 + \Gamma_3 + \Gamma_4$
4	$\Gamma_1 + \Gamma_2 + 2\Gamma_3 + 2\Gamma_4$
5	Γ_1

J_x M	0	1	2	3	4	5	6	7	8	9	10	11	12	13	14	15
0.75	Γ_2	Γ_1	Γ_2	Γ_1	Γ_4	Γ_2	Γ_4	Γ_3	Γ_3	Γ_4	Γ_2	Γ_4	Γ_3	Γ_3	Γ_4	Γ_1
0.6	Γ_2	Γ_1	Γ_2	Γ_1	Γ_3		Γ_4	Γ_3	Γ_3	Γ_4	Γ_1	Γ_4	Γ_3	Γ_3	Γ_4	Γ_1
0.3	Γ_2	Γ_1	Γ_2	Γ_1							Γ_1	Γ_4	Γ_3	Γ_3	Γ_4	Γ_1

The quantum mechanical magnetization curves for $S = 3$ are also shown in figures 7–9. As can be seen the quantum magnetization curves consist of a series of steps of height $1/S$ or some integer multiple of this. Apart from this discreteness the quantum curves are similar to the classical ones, reflecting the fact that $S = 3$ is already fairly large.

The irreducible representations of the states corresponding to each horizontal part of the curve are given in the following table. A blank indicates that the magnetization with that value does not occur.

Again for each region we find that the representations of the lowest quantum states are a subset of the classical representations. Just as for the triangle and tetrahedron the full classical representation is obtained by considering both integer and integer $+\frac{1}{2}$ spins and considering low-lying states which become degenerate with the lowest state in the limit $S \to \infty$. Our speculation in the earlier paper [2] that the pattern in region 4 is of period 10 we now believe to be incorrect, the correct pattern being of period 5, corresponding to the regular representation.

Note that region 3 is so narrow as a function of B that we cannot obtain meaningful results for the quantum case.

5. Other clusters

In this paper we have concentrated on small symmetric clusters in which the interaction is frustrated, i.e. nearest-neighbour paths of odd length exist. We have also looked at unfrustrated clusters, e.g. a pair of atoms and rings of even numbers of atoms. The behaviour for all of these is very similar to that of a pair of atoms. In the lowest states alternate atoms are always parallel and effectively act as a single spin. The anisotropic exchange merely introduces a single step in the magnetization curve at low field for $J_x < J_z$, and it is continuous if $J_x > J_z$. An octahedron behaves very much like a triangle since opposite spins are always parallel and behave as a single spin in the lowest states.

The extension of these ideas, including anisotropy, to the larger clusters considered in [1] and to models of the more complicated structures found experimentally is straightforward although more lengthy and is being studied in a few of the more interesting cases.

6. Conclusion

The inclusion of anisotropy in the exchange interaction has had two effects. One is to make the $T = 0$ phase structures much more complicated and interesting. The other is that the extra detailed information has enabled us to establish clearly the symmetry properties of the classical clusters in terms of the irreducible representations of the space groups. Also we have seen how the quantum systems typically have steps of higher symmetry but overall tend to the classical result at large S, as expected.

However, we still do not have a complete description of the symmetry since the space group only distinguishes between spins with *different* orientations. It does not take into account the fact that the spin directions may be related. For example, for the five-atom ring, in region 4 the spins are all different but are related by a rotation about the z-axis of $4\pi/5$. Also regions 2 and 3 have the same space group symmetry but clearly have different spin symmetries.

Some further information can be obtained by considering the 'magnetic group' where the space and spin components are transformed by the same operations. It therefore involves only the intersection of the space group and spin groups, which in turn depends on the direction of the field and axis of anisotropy. If this is taken perpendicular to the plane of the triangle or pentagon the group is C_3 or C_5 respectively. Reducing the spin-space product representations correctly predicts that completely invariant spin structures like the fans should occur as found in region 5 of the triangle. The predictions for other regions are less specific but consistent with the classical structures. Further study of these is planned.

References

[1] Parkinson J B and Timonen J 2000 *J. Phys.: Condens. Matter* **12** 8669–82
[2] Parkinson J B, Elliott R J, Timonen J and Viitala E 2002 *J. Phys.: Condens. Matter* **14** 45–58
[3] Bates C A and Jasper R F 1971 *J. Phys. C: Solid State Phys.* **4** 2330–40

[4] Rawson J M and Winpenny R E P 1995 *Coord. Chem. Rev.* **139** 313–74
[5] Winpenny R E P 1998 *Chem. Soc. Rev.* **27** 447–52
[6] Thomas L, Lionti F, Ballou R, Gatteschi D, Sessoli R and Barbara B 1996 *Nature* **383** 145–7
Friedman J R, Sarachik M P, Tejada D and Ziolo R 1996 *Phys. Rev. Lett.* **76** 3830–3
[7] Barbara B, Thomas L, Lionti F, Chiorescu I and Sulpice A 1999 *J. Magn. Magn. Mater.* **200** 167–81
Barbara B and Gunther L 1999 *Phys. World* **12** 35
[8] Chiorescu I, Giraud R, Jansen A G M, Caneschi A and Barbara B 2000 *Phys. Rev. Lett.* **85** 4807–10
[9] Giraud R, Wernsdorfer W, Tkachuk A M, Mailly D and Barbara B 2001 *Phys. Rev. Lett.* **87** 057203
[10] Müller A and Döring J 1991 *Angew. Chem. Int. Edn Engl.* **27** 1721
Gatteschi D, Pardi L, Barra A L, Müller A and Döring J 1991 *Nature* **354** 463–5
Gatteschi D, Pardi L, Barra A L and Müller A 1993 *Mol. Eng.* **3** 157–69
[11] Chiorescu I, Wernsdorfer W, Müller A, Bögge H and Barbara B 2000 *J. Magn. Magn. Mater.* **221** 103–9
[12] Chiorescu I, Wernsdorfer W, Müller A, Bögge H and Barbara B 2000 *Phys. Rev. Lett.* **84** 3454–7
[13] Brinkman W F and Elliott R J 1966 *Proc. R. Soc.* A **294** 343–58
[14] Altmann S L and Herzig P 1994 *Point-Group Theory Tables* (Oxford: Clarendon)
[15] Oshikawa M, Yamanaka M and Affleck I 1997 *Phys. Rev. Lett.* **78** 1984–7
[16] *Numerical Recipes* 1986 (Cambridge: Cambridge University Press) chapter 10